JOURNAL OF GEOPHYSICAL RESEARCH, VOL. 114, F03022, doi:10.1029/2008JF001139, 2009

Importance of wind conditions, fetch, and water levels on wave-generated shear stresses in shallow intertidal basins

S. Fagherazzi[1] and P. L. Wiberg[2]

Received 19 August 2008; revised 24 June 2009; accepted 7 July 2009; published 30 September 2009.

[1] Wave-generated shear stresses are the main mechanism responsible for sediment erosion on tidal flats and regulate both sediment concentrations in the water column and, together with tidal currents, sediment export to salt marshes and to the ocean. We present herein a simple method to estimate sediment erosion potential in shallow tidal basins caused by wind wave events. The method determines the aggregate response of the entire basin, combining in a simple framework the contribution from different landscape units. The method is applied to a system of shallow tidal basins along the Eastern Shore of Virginia, USA. Our analysis unravels the interplay of basin morphology, tidal elevation, and wind direction on water depth, fetch, and the resulting wave-generated shear stresses. We identify four bottom shear stress regimes as a function of water elevation produced by wind waves in shallow micromesotidal systems. For water elevations below mean lower low water (MLLW), an increase in fetch is counteracted by an increase in depth, so that the average bottom shear stress and erosion potential is maintained constant. For elevations between MLLW and mean sea level (MSL), the increase in water depth dominates the increase in wave height, thus reducing the bottom shear stresses. For elevations between MSL and mean higher high water (MHHW), the range associated with stable salt marsh platforms, flooding of salt marshes increases fetch, wave height, and bottom shear stresses, producing the largest resuspension events in the bay. For elevations above MHHW, the increase in depth once again dominates increases in wave height, thereby reducing average bottom shear stresses and potential erosion.

Citation: Fagherazzi, S., and P. L. Wiberg (2009), Importance of wind conditions, fetch, and water levels on wave-generated shear stresses in shallow intertidal basins, *J. Geophys. Res.*, *114*, F03022, doi:10.1029/2008JF001139.

1. Introduction

[2] Wind waves and the bed shear stresses they produce are critical for the morphological and ecological equilibrium of shallow tidal basins. Wave-generated shear stresses are the main mechanism responsible for sediment erosion on tidal flats and regulate both sediment concentration in the water column and hence light availability at the bed [e.g., *Lawson et al.*, 2007] and, together with tidal currents, sediment export to salt marshes and to the ocean. Wind waves also have an important influence on sediment budgets in the intertidal zone, which ultimately determine the morphological evolution of tidal basins [e.g., *Tambroni and Seminara*, 2006; *Fagherazzi and Overeem*, 2007]. Moreover, shear stresses produced by wind waves strongly affect sea grasses [*Fonseca and Bell*, 1998; *Ramage and Schiel*, 1999], biogeochemical cycles within the bottom sediments [*Precht and Huettel*, 2003; *Precht et al.*, 2004] and biofilms at the sediment surface [*Amos et al.*, 2004]. In particular, large wave-generated shear stresses can break or remove the biofilm at the bottom surface, rework the top layer of sediments increasing the chemical exchanges with the ocean water, and disturb sea grass canopies and macroalgal mats. Finally, wind waves are a main cause of salt marsh deterioration through scarp erosion [*Möller et al.*, 1996, 1999].

[3] The response of a shallow tidal basin to wind events and the related distribution of bottom shear stresses are strongly dictated by the morphology of the intertidal landscape, the distribution of channels, salt marshes, and tidal flats in the basin in relation to water depth [*Fagherazzi et al.*, 2006; *Defina et al.*, 2007]. Wave generation depends on transfer of energy from the wind to the water surface, which is a function of fetch (the unobstructed distance over which the wind can blow), water depth and duration of the wind events. Emergent salt marshes and other intertidal landforms strongly influence wind fetch. During low-tide conditions, emergent land surface reduces the extent of open water and hence the fetch, limiting the maximum wave height produced by storms. During high-tide conditions, subbasins within a shallow tidal system may become connected, significantly increasing maximum fetch.

[4] Intertidal landscape complexity and water depths are subject to a variety of drivers and disturbances in addition to tides, including storm surges, sea level rise, changes in sediment supply and anthropogenic modifications of the

[1]Department of Earth Sciences and Center for Computational Science, Boston University, Boston, Massachusetts, USA.
[2]Department of Environmental Sciences, University of Virginia, Charlottesville, Virginia, USA.

0148-0227/09/2008JF001139$09.00

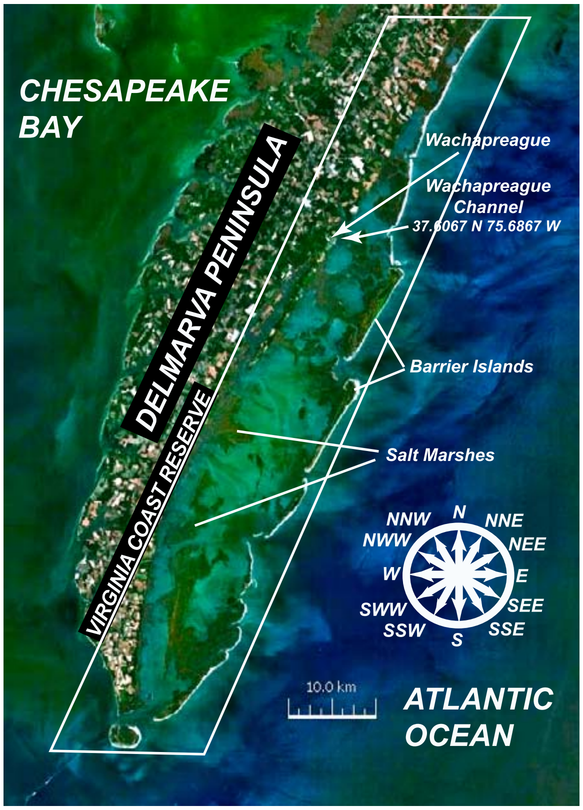

Figure 1. Study site: Virginia Coast Reserve, Eastern Shore, Virginia, USA (courtesy NASA World Wind).

coastline [*Fitzgerald et al.*, 2008]. To assess the impact of these drivers on shallow tidal basins, it is useful to take an integrated approach in which the response of the entire basin is determined as a function of the processes at play. This holistic approach is already successfully applied to terrestrial watersheds, in which denudation rates, water runoff, and sediment fluxes are aggregated at the catchment scale to provide the global response of the system under different scenarios [*Rodriguez-Iturbe and Rinaldo*, 1997], but it is still relatively novel in marine and coastal environments [see also *Tambroni and Seminara*, 2006].

[5] Herein we present a method to analyze the response of a system of shallow tidal basins to wind wave events, with a specific focus on the interplay of basin morphology, water elevation and wind direction on depth, fetch and the resulting wave-generated shear stresses. Our goal is to determine the aggregate response of intertidal basins in terms of erosion potential, combining in a simple framework the contribution from different landscape units. We apply our method to a system of shallow lagoons and salt marshes behind the barrier islands along the Eastern Shore of Virginia, a setting typical of many shallow barrier systems. This application leads us to a general conceptual understanding of the relative importance of fetch and water depth in controlling wave-generated bottom shear stresses and erosion potential in shallow coastal bays with emergent salt marshes. Our method and results, which provide critical insight into the feedbacks between landforms and sediment fluxes in intertidal areas, can readily be applied to other shallow tidal basins.

2. Study Site

[6] Our study site is in the Virginia Coast Reserve (VCR), located on the Atlantic side of the Delmarva Peninsula (Figure 1). The VCR includes a number of shallow lagoons bordered by *Spartina alterniflora* marshes both on the mainland and the barrier islands (Figure 1); marsh islands are also present within the lagoons. About 50% of the lagoon area is less than 1 m deep at mean low water [*Oertel*, 2001; sites deeper than a few meters are limited to the large tidal channels that cut through the lagoons. The lagoons comprise intertidal and subtidal basins located between the barrier islands and the Delmarva Peninsula. Each basin is connected to the Atlantic Ocean through a tidal inlet. The VCR is typical of shallow coastal barrier-lagoon-marsh systems that dominate the Atlantic and Gulf coasts.

[7] Tides are semidiurnal, with a mean tidal range of 1.2 m. Mean higher high water (MHHW) at Wachapreague channel (NOAA station 8631044 (Figure 1)) is 0.68 m above mean sea level, whereas mean lower low (MLLW) water is -0.70 m and mean low water is -0.65 m with respect to mean sea level. At this station mean sea level (MSL) is 1.40 m above station datum (NAVD88). During storm surges both high water and low water can be modified, depending on wind intensity and direction. The highest water level on record is 2.02 m above MSL, (5 February 1998) whereas the lowest is -1.56 m above MSL (16 March 1980). The current rate of relative sea level rise in the region is 3.8–4.0 mm yr^{-1} (tidesandcurrents.noaa.gov). Storms are the primary agent of short-term disturbance in this coastal region. On average, more than 20 extratropical storms rework the landscape each year [*Hayden et al.*, 1995]. Marsh vegetation on the intertidal (low) salt marshes bordering the lagoons is dominated by *Spartina alterniflora*, with an average stem height of 30 cm and a height range between 50 and 100 cm.

[8] The shallow depths of the VCR make lagoon bottom sediment ($D_{50} \approx 63$ μm with sorting coefficient $\sqrt{D_{84}/D_{50}} \approx$ 2) susceptible to wind-driven waves and currents, thus promoting sediment resuspension [*Lawson*, 2004; *Lawson et al.*, 2007]; tides alone are generally insufficient to resuspend sediment from the lagoon bottom. Wind speed measured at an offshore buoy 30 km southeast of the southern tip of the Delmarva Peninsula (NDBC buoy CHLV2; anemometer height is 43 m above mean sea level; www.ndbc.noaa.gov) averaged 7.5 ± 3.8 (SD) m s^{-1} from 1988 to 2007. The dominant wind directions are from the SSE-SSW and N-NE; the highest winds tend to come from a northerly quadrant between NW and NE (Figure 2). Wind events are possible in any season, but are more frequent and have higher wind speeds in winter.

[9] The hypsometric curve for the whole system of lagoons is reported in Figure 3. Most of the basin area is located between -2 m and 0.5 m above MSL, and marsh elevation is typically 0.3 m above MSL. The distribution of elevations at the Virginia Coast Reserve is typical of shallow intertidal basins delimited by barrier islands, as, for example, the Venice Lagoon, Italy [*Fagherazzi et al.*, 1999], Plum Island Sound, Massachusetts [*Vallino and Hopkinson*,

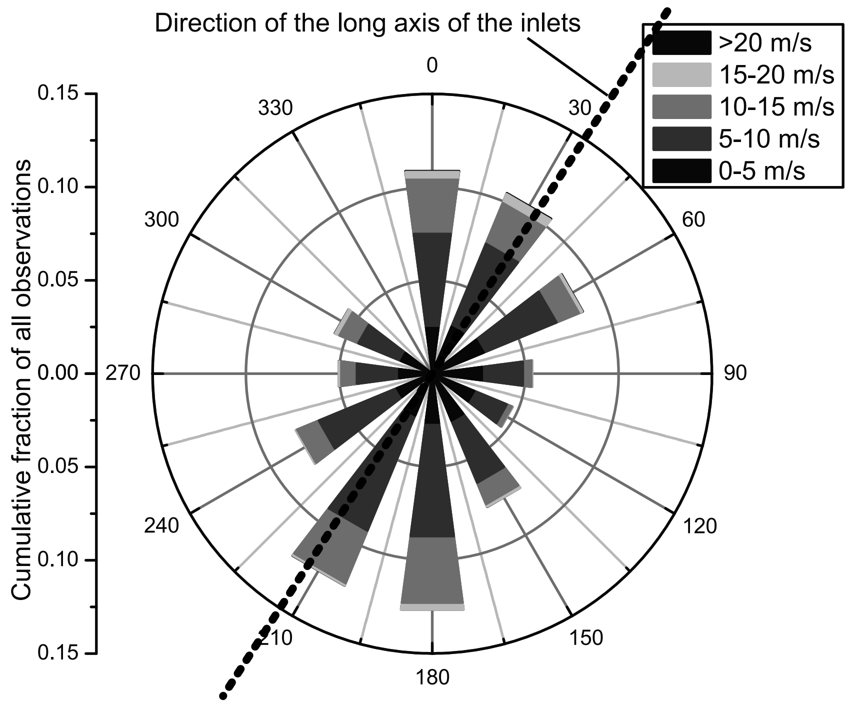

Figure 2. Directional distribution of winds in the study area, binned by speed, from 1988 to 2007. Wind data are from NDBC buoy CHLV2, located 30 km southeast of the southern tip of the Delmarva Peninsula.

1998], Barataria Bay, Louisiana [*Fitzgerald et al.*, 2004] and Apalachicola Bay, Florida [*Huang et al.*, 2002]. All these lagoons are characterized by deep channels, shallow tidal flats, and emergent salt marshes. Therefore the conceptual results presented herein are of general validity, and can readily be applied to tidal environments like these.

3. Distribution of Fetch and Water Depth as a Function of Tidal Elevation

[10] In order to study the distribution of bottom shear stresses produced by wind waves, we first analyze the distribution of fetch and water depth in the shallow tidal basins that form the Virginia Coast Reserve, since these two parameters, together with wind speed, determine wave height at each basin location [e.g., *Young and Verhagen*, 1996a].

[11] Basin area is a strong function of water surface elevation. When surface elevations are higher than 0.3 m above mean sea level (the datum for all elevations provided here) most of the basin is covered by water. Here we compute basin area on the basis of bare earth surfaces, neglecting emergent vegetation which would also influence wind speed and fetch; the effects of vegetation will be considered later. For water surface elevations between 0.3 and −0.9 m, salt marshes and some intertidal shoals emerge, reducing the extent of continuous open water in the basin. Below −0.9 m, even the tidal flats become emergent and only deep channels remain submerged (Figure 4).

[12] This distribution of landforms within the basins dictates the distribution of fetch, taken as the unobstructed length over which the wind can blow. To analyze the fetch and depth distribution at the VCR, we utilize a Digital Elevation Model (DEM) with a 200 m element size derived from available bathymetric data. We define fetch for any given water surface elevation as the distance between a DEM element where we want to compute the wave height and the closest emergent element along a determined direction. We then determine the distribution of fetch for every wind direction by computing the fetch for every DEM element below the water surface.

[13] The distribution of fetch for every point of the basin strongly depends on wind direction. For water elevations above 0.6 m, wind can blow over the entire basin; the maximum fetch of 50 km occurs for winds from NNE and SSW, parallel to the barrier islands and along the major dimension of the tidal basin (Figures 5 and 1). The directions producing the second highest fetches are N-S, whereas the smallest fetches occur for wind directions perpendicular

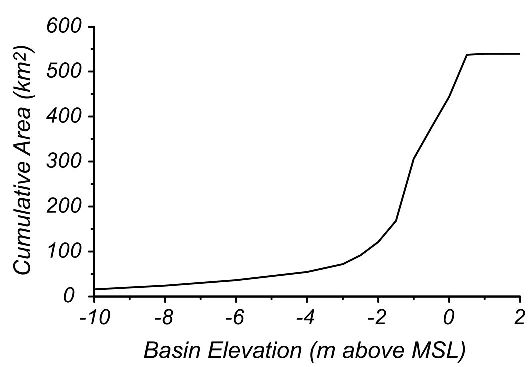

Figure 3. Hypsometric curve of the Virginia Coast Reserve shallow lagoons.

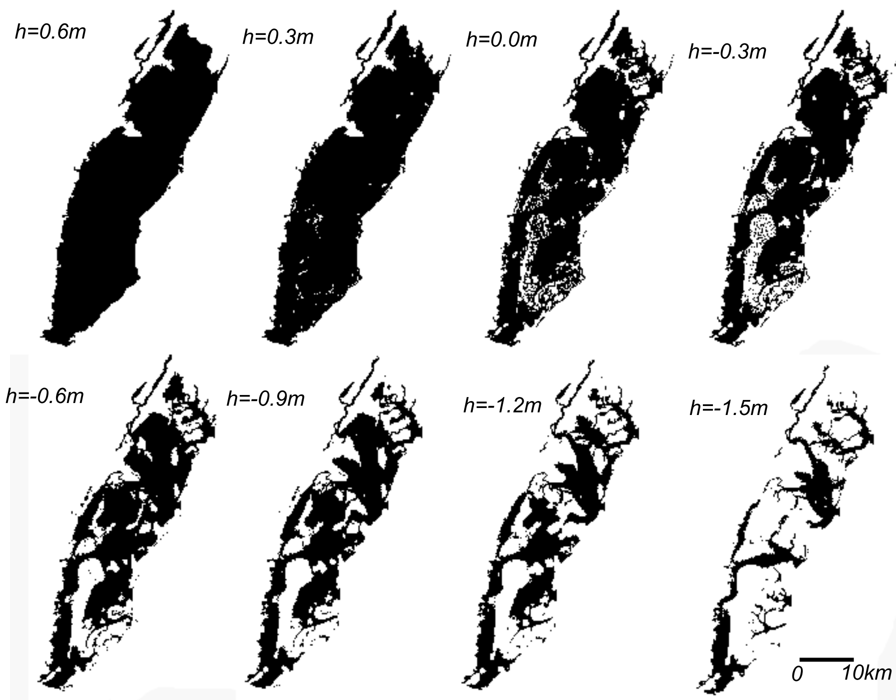

Figure 4. Tidal basin areas below water (in black) for different sea level elevations, indicated as height above mean sea level. The bathymetry has a grid spacing of 200 m.

to the barrier islands, from WNW-ESE. For a water elevation below MSL the N–S directions produce the highest fetches since emergent salt marshes limit the fetch along the NNE-SSW (Figure 5). Regardless of wind direction, fetch decreases rapidly with decreasing water elevations for elevations above MSL, though the change in fetch is most dramatic for NNE and SSW winds. Once water elevations are below MSL, fetch decreases more slowly as elevation drops, with relatively little dependence on wind direction.

[14] In addition to fetch, water depth is a major control on the height of wind-generated waves in shallow basins. Therefore, for each wind direction, we analyze the average water depth along the fetch for each DEM element in the basin (Figure 6). To eliminate a disproportionate influence of deep channels on the statistics we reduce channel depths to 2 m, the average elevation of the bordering tidal flats (Figure 3). Moreover, for the computation of waves on the marsh platform we use the actual water depth rather than the average water depth along the fetch.

[15] The distribution of average depths is not very sensitive to direction, though the average depth for ENE and NNE fetches is smaller than for ESE and SSE fetches because the southern part of the tidal basin is on average shallower. This trend in depth influences the overall depth distribution because when winds blow from ENE and NNE, the fetch always contains points in the southern part of the basin, thus reducing the fetch-averaged depth. We therefore

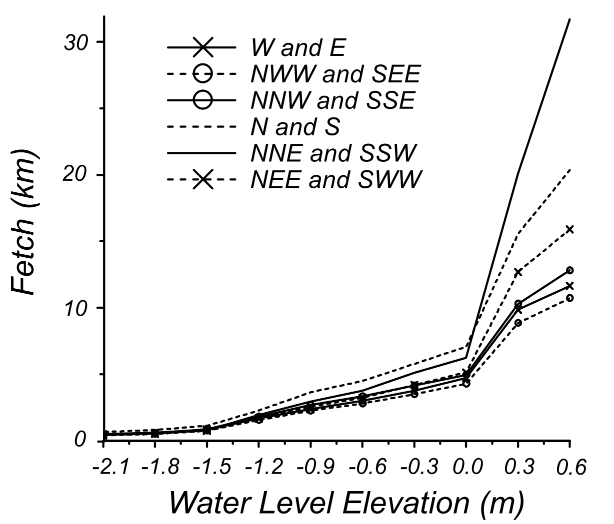

Figure 5. Average fetch length for every submerged point as a function of water elevation above mean sea level.

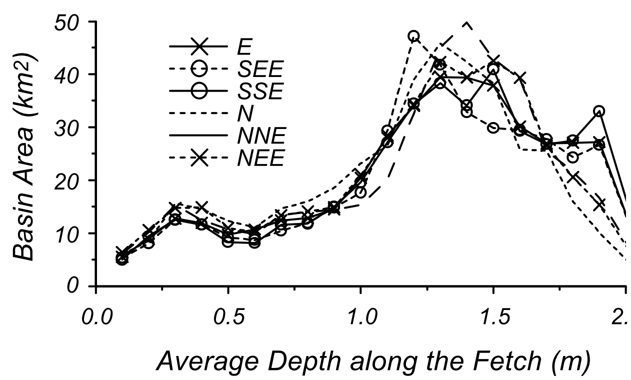

Figure 6. Distribution of average water depth along the fetch for each wind direction; water elevation is mean sea level. The distribution is plotted as a continuous line for visualization purposes; the depth data are binned every 0.1 m.

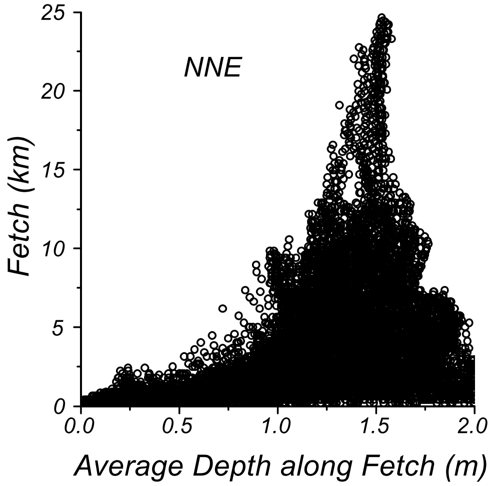

Figure 7. Relationship between depth and fetch for every point of the basin for a water level equal to MSL and a wind direction from NNE.

expect slightly lower wave heights for winds blowing from the south for a given fetch distance. Fetch-averaged depth varies with water elevation (e.g., tidal phase), but differences among different wind directions are similar to the ones shown in Figure 6.

[16] Fetch and average depth are not independent variables. Deep areas (depth >2.0 m) are limited in extent, so that large average depths are related only to small fetches (Figure 7). Similarly, very shallow areas (depth <1.0 m) are also limited in extent, so that the highest fetch values typically occur for average depths between 1.0 and 2.0 m. It is important to note that the average depth along the fetch is reduced by the truncation of channel depths at 2.0 m.

4. Fetch-Limited Waves in Water of Finite Depth and Related Shear Stresses

[17] Waves evolve differently in shallow water compared to deep-water conditions. At short fetch, wave heights are comparable, but as fetch increases, wave growth is reduced with respect to deep water conditions, and peak frequency shifts to higher values relative to deep-water wave growth.

[18] In contrast to wave evolution in deep water [e.g., *Hasselmann et al.*, 1973], data describing fetch-limited wave growth in shallow depths are scarce. *Thijsse* [1949] was the first to study shallow water wave growth whereas the first comprehensive field investigation was staged in Lake Okeechobee by *Bretschneider* [1958] and *U.S. Army Corps of Engineers* [1955], from which a set equations linking wave energy and wave period to fetch and average depth were developed [*Coastal Engineering Research Center* (*CERC*), 1984].

[19] Herein we use the formulation presented by *Young and Verhagen* [1996a, 1996b], which is similar to the *CERC* [1984] formulation but takes in account the results of a full-scale experiment in Lake George, Australia, whose depth is comparable to the average depth of the Virginia Coast Reserve. We chose this formulation because it represents, together with the one reported by *CERC* [1984], the state-of-the-art of analytical methods for wave height prediction in shallow water. Recent advanced numerical models for wave propagation (e.g., SWAN [*Booji et al.*, 1999]) use the same functional relationship between fetch, depth and wind speed as these early analytical approximations.

[20] Following the results of *Young and Verhagen* [1996a], the nondimensional wave energy $\epsilon = g^2E/U^4$ and the nondimensional peak frequency $\nu = fU/g$ are related to the nondimensional fetch $\chi = gx/U^2$ and the nondimensional water depth $\delta = gd/U^2$ through the expressions:

$$\varepsilon = 3.64 \times 10^{-3} \left\{ \tanh A_1 \tanh \left[\frac{B_1}{\tanh A_1} \right] \right\}^{1.74} \tag{1}$$

where g is gravitational acceleration, E is wave energy, U is the reference wind velocity at an elevation of 10 m, f is wave frequency, x is fetch, d is water depth and

$$A_1 = 0.493\delta^{0.75} \tag{2}$$

$$B_1 = 3.13 \times 10^{-3}\chi^{0.57} \tag{3}$$

and

$$\nu = 0.133 \left\{ \tanh A_2 \tanh \left[\frac{B_2}{\tanh A_2} \right] \right\}^{-0.37} \tag{4}$$

where

$$A_2 = 0.331\delta^{1.01} \tag{5}$$

$$B_2 = 5.215 \times 10^{-4}\chi^{0.73} \tag{6}$$

[21] We can calculate wave height, H, from wave energy through the expression $E = \rho g H^2/8$. Here, we have limited our analysis to monochromatic waves since the complexity of the basin bathymetry would probably prevent a correct description of wave generation and evolution through a complete spectral analysis and our goal is to keep the model as simple as possible. The maximum velocity of wave-induced water motion at the bottom can be evaluated using linear wave theory:

$$u_b = \frac{\pi H}{T \sinh(kd)} \tag{7}$$

and bottom shear stress is given by

$$\tau = \frac{1}{2} f_w \rho u_b^2 \text{ with } f_w = 0.04 \left[\frac{u_b T}{2\pi k_b} \right]^{-0.25} \tag{8}$$

where T is wave period, k is wave number, ρ is water density, and f_w is a friction factor that depends on the roughness length scale of the sediment bed k_b [*Fredsoe and Deigaard*, 1993]. Herein, we let $k_b = 2D_{90}$ [e.g., *Kamphuis*, 1975], so that equation (8) estimates the skin friction stress, and set D_{90} = 0.25 mm on the basis of grain size data from Hog Island Bay (Figure 1 [*Lawson*, 2008]). The wave number k can be determined from the dispersion equation derived from the wave linear theory:

$$\sigma = \sqrt{gk \tanh(kd)} \tag{9}$$

where $\sigma = 2\pi/T$ is wave frequency.

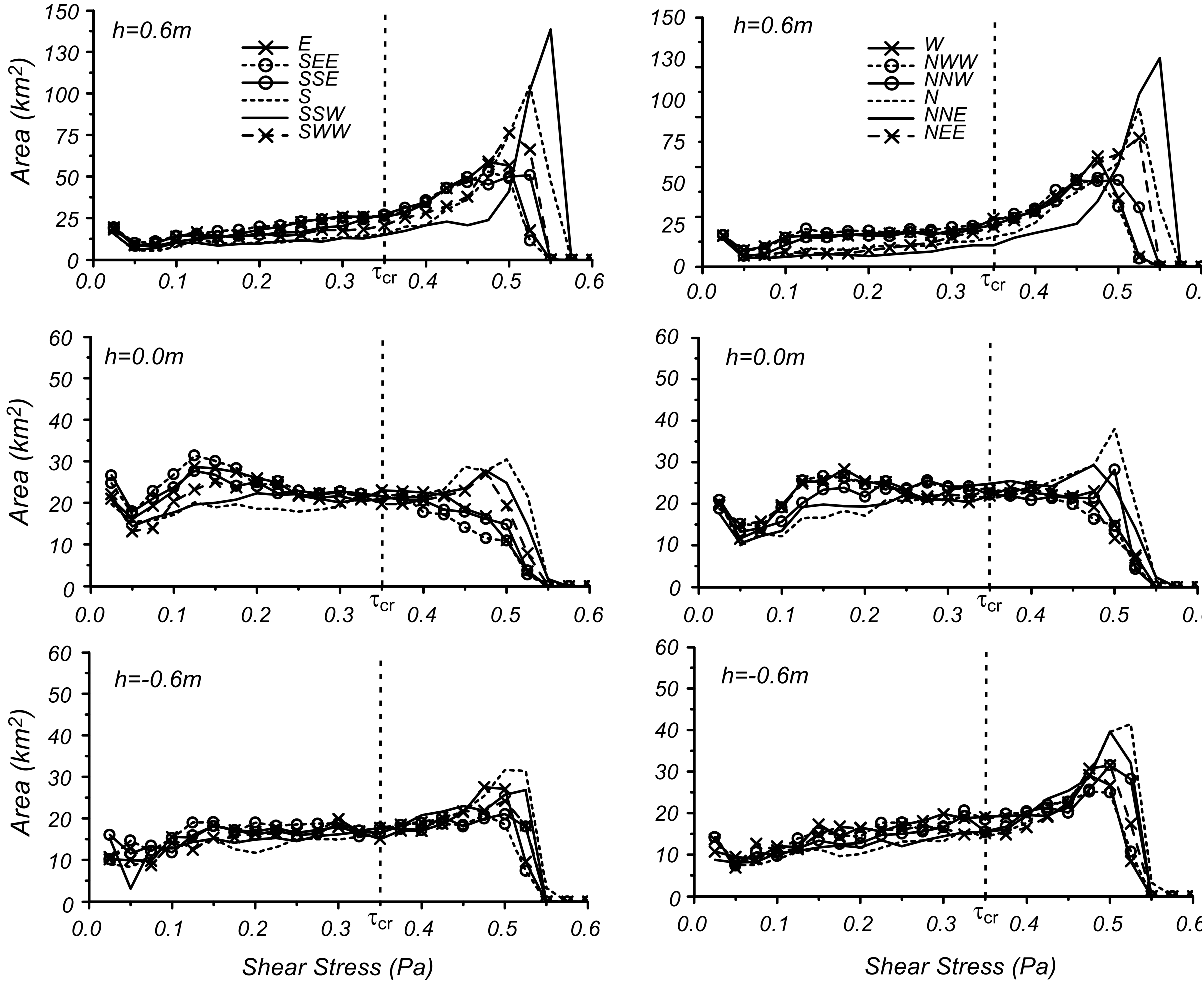

Figure 8. Distribution of shear stresses produced by a wind of 15 m s^{-1} for different directions and water elevations. The distribution is plotted as a continuous line for visualization purposes; the shear stress data are binned every 0.25 Pa.

[22] The distribution of shear stresses at the basin bottom calculated using equations (1)–(9) depends on wind intensity, direction, and water elevation. In Figure 8 we report the distributions produced by a wind of 15 m s^{-1} (the 96th percentile of wind speed from 1988 to 2007 at NOAA buoy CHLV2 (see Figure 2)). We chose this wind speed because it is frequent enough to be geomorphologically significant for the tidal basin but large enough to produce wind waves capable of resuspending lagoon bottom sediment. It is interesting to note that for a given water elevation, the distribution of shear stress among the various wind directions differs most for large shear stresses, which are the most effective in resuspending sediment. The maximum bottom shear stresses are similar for every wind direction, showing that the basin dimensions are sufficient to reach fetch unlimited conditions for at least a small portion of the lagoon. However, the distribution of area as a function of shear stress, particularly the total area affected by high waves, changes considerably as wind direction varies.

[23] For water levels above the average marsh elevation (~0.3 m) and for winds blowing from SSW-NNE, the mode of the shear stress distribution is above 0.5 Pa. For water elevations below the marsh elevation (~0.3 m), the highest shear stresses are reached for winds blowing from the north, since the emergent salt marshes limit the fetch in the NNE-SWW direction. For water elevations below mean sea level (~0.0 m) the average shear stress is slightly higher for wind directions from the north rather than from the south, since the southern part of the basin is shallower thus reducing the total wave height.

[24] To determine the response, in terms of sediment erosion potential, of the entire basin to a specific wind condition, we need to account for both wind wave-generated bottom shear stress and total area influenced by each specific shear stress. We therefore define an erosion factor EF equal to

$$EF = \sum_i A_i(\tau_i - \tau_{cr}) \tag{10}$$

where τ_i is the bottom shear stress at a location i which has an area equal to A_i and τ_{cr} is a suitable value of critical shear stress for bottom erosion. We set τ_{cr} = 0.35 Pa on the basis of measurements and modeling of sediment erosion and resuspension in the study area [*Lawson*, 2008]. Critical shear stresses in shallow lagoonal systems can vary from 0.2 Pa for

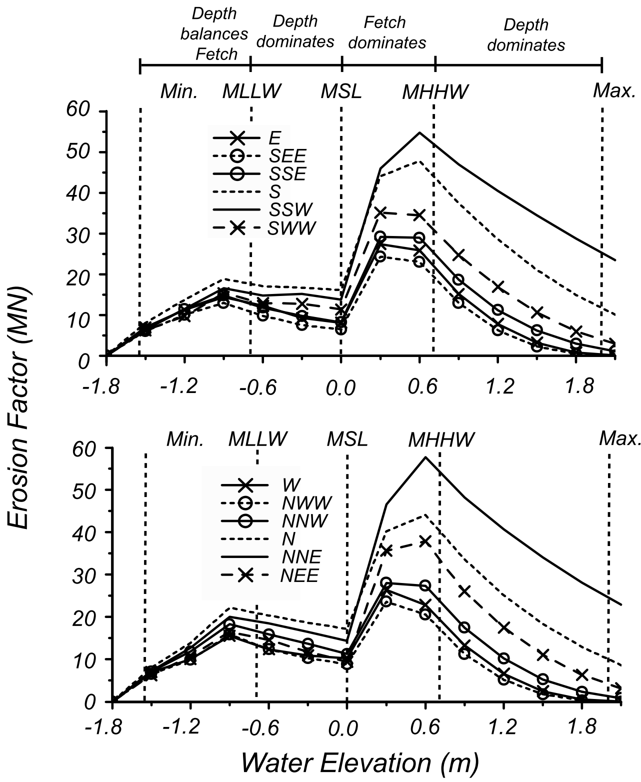

Figure 9. Erosion factor (equation (10)) for a wind of 15 m s^{-1} as a function of water depth and wind direction.

noncohesive sediments to 1 Pa or more for high-density cohesive sediments with biofilms [*Amos et al.*, 2004]. Erosion rates for cohesive sediments are directly proportional to the difference between actual and critical shear stress [*Sanford and Maa*, 2001], while for noncohesive sediments the erosion rates are proportional to this difference to a power that ranges between 1.5 and 2. Clay content in bed sediment in Hog Island Bay (Figure 1) ranges from 4 to 40% by mass, and direct measurements of sediment erosion at sites across Hog Island Bay display the form characteristic of cohesive sediment erosion [*Lawson*, 2008]. Bottom sediment in the other lagoons of the VCR is similar to that in Hog Island Bay, thus we can use the erosion factor (equation (10)) as a simple index to estimate the response of the entire basin to wind-generated waves.

[25] In Figure 9 we plot the erosion factor as a function of water elevation in the basin for a wind speed of 15 m s^{-1} blowing from different directions. The erosion factor grows as water elevations submerge the marshes ($\sim$0.3 m above MSL) leading to higher fetches. Under these conditions the differences among different wind directions are consistent, with winds from N-S and NNE-SSW producing the highest erosion. For water elevations above $\sim$0.6 m (near MHHW), bottom shear stresses decrease despite the higher waves because the water is too deep to feel the influence of the waves (wave orbital velocities decay exponentially with depth). The peak in erosion factor varies with wind direction, showing that it is controlled by fetch distribution, but the location of the peak does not change with wind speed.

[26] The erosion factor is smaller when the salt marshes are emergent, for water elevations <0.3 m, because of a reduction in basin area and fetch. A decrease in water elevation from MSL to -0.9 m (<MLLW) leads to a modest increase in the erosion factor, despite a decrease in fetch and submerged area, because bottom shear stresses are higher in shallower water depths for the same wave height and period. Between MSL and MLLW, the highest erosion factor occurs for winds from the north and NNE.

[27] The erosion factor in Figure 9 was calculated without accounting for the wave dissipation produced by halophyte vegetation on the marsh platform. *Möller et al.* [1999], for example, measured an average wave dissipation of 60% along 200 m of vegetated salt marsh in Norfolk, England [see also *Knutson et al.*, 1982]. To test the influence of vegetation on bottom shear stresses we assume that all surfaces above MSL are vegetated and we compute wave attenuation with the equation

$$E = E_0 e^{-kx} \tag{11}$$

where E_0 is the incoming wave energy and E is the wave energy after dissipation along a distance x of marsh platform. The dissipation rate k is set equal to 7.1 km^{-1} in accordance with the data presented by *Möller et al.* [1999]. The distance x is computed from the DEM considering only the marsh platform along the wind direction. It is important to note that the dissipation rate is also a function of water depth, so that the average value computed in equation (11) overestimates dissipation for large water depths on the marsh platform and underestimates it for small water depths. Nonetheless, equation (11) represents a good first-order approximation of wave dissipation due to vegetation on submerged marshes.

[28] The influence of marsh vegetation is evident in a modest reduction of the erosion factor for water elevations above MSL, though it still displays a marked maximum for elevations between 0.3 m and 0.6 m ($\sim$MHHW) (Figure 10). Simulations with higher wave dissipation on the marshes do not change the erosion factor much (difference less than 2%), indicating that most of the erosion producing the peak in Figure 10 occurs on the unvegetated tidal flats.

[29] By plotting submerged area, average fetch, average depth, average wave height, and average bottom shear stress, accounting for effects of marsh vegetation, as a function of water elevation (Figure 11) for a wind blowing from the north with a speed of 15 m s^{-1}, we notice that the

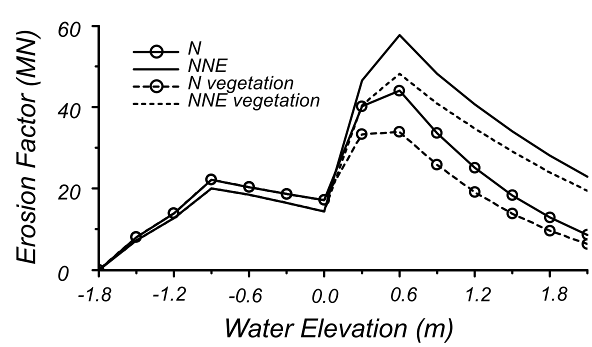

Figure 10. Comparison of erosion factor with and without the influence of marsh vegetation on wave attenuation for 15 m s^{-1} winds blowing from the north and NNE.

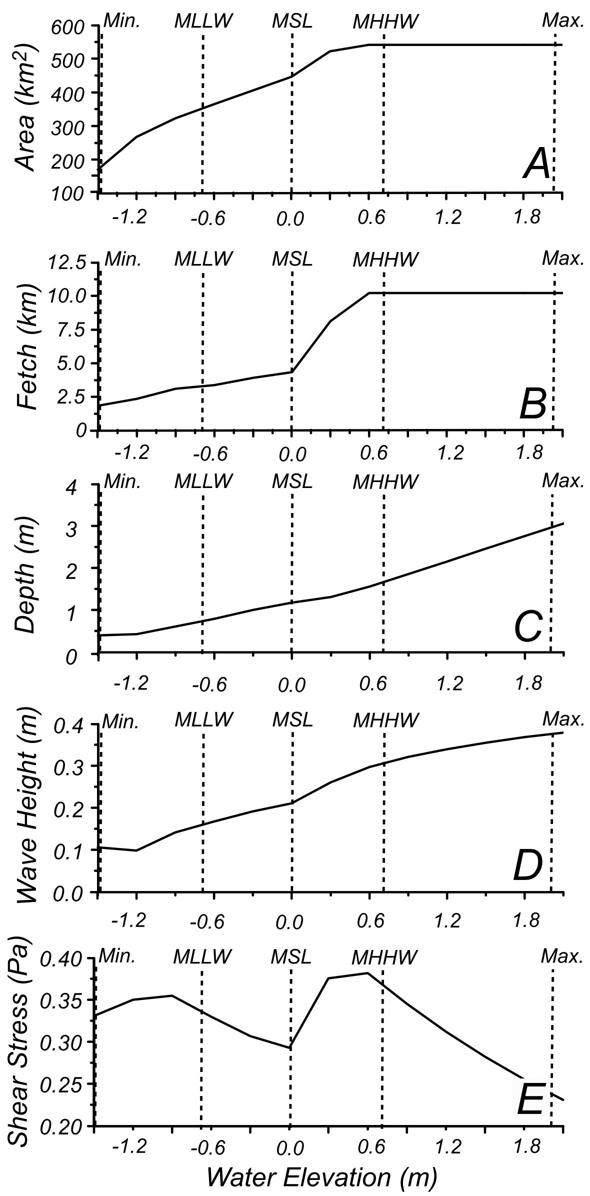

Figure 11. (a) Basin area, (b) average fetch, (c) average depth, (d) average wave height, and (e) average bottom shear stress as a function of water elevation for a wind blowing from north with a speed of 15 m s^{-1}.

submerged area linearly increases until the salt marshes are submerged. The average fetch slowly increases for lower elevations (below MSL) but rapidly increases between MSL and MHHW as the salt marshes are flooded. In contrast, average water depth increases steadily with an increase in water elevation. As a consequence, wave height increases monotonically with elevation, since both water depth and fetch increase. Below MLLW, an increase in water depth is counteracted by an increase in wave height, thus producing an almost constant average bottom shear stress (Figure 11e). Between MLLW and MSL, depth increases faster than wave height so that shear stress decreases (Figure 11e). Fetch rapidly increases between MSL and MHHW as the salt marshes are inundated and the basin becomes more continuous. The increase in fetch produces higher waves that increase the potential erosion on the tidal flats. As a consequence, bottom shear stress consistently grows between MSL and MHHW, producing the peak in erosion factor reported in Figure 9. For water elevations greater than MHHW, fetch is constant and wave height once again increases more slowly than water depth, thus reducing the average bottom shear stress.

[30] Because wave height (and therefore wave orbital velocity), bed shear stress and the erosion factor grow monotonically with wind speed, the erosion factor should be qualitatively similar for different wind speeds (Figure 12, for winds blowing from the north). The highest erosion factors are registered when the salt marshes are just submerged (water elevation 0.3 m). Under these conditions most of the erosion takes place on the tidal flats, with negligible effect on the marsh surface.

5. Meteorological Controls on Water Level

[31] Because wind speed, direction and water depth are all important controls on wave-generated bed shear stresses and erosion factors (e.g., Figures 9 and 12), it is important to understand the degree to which water levels depend on wind speed and direction. Significant correlations between wind speed and direction will increase erosion potential during northeasterly storms by maximizing the fetch over which the wind blows when water levels are in the range of 0.2–1.0 m above MSL (Figure 9). On the other hand, if the highest water levels are associated with strong northeasterly winds, the resulting energetic wave conditions will produce limited resuspension over much of the basin at times when average water depth is sufficiently large that wave orbital motion decays before reaching the bottom.

[32] Measured flood tide peak water levels at Wachapreague, Virginia (Figure 1), exhibit a broader range of values than predicted flood tide levels, largely as a result of meteorological conditions (Figure 13, left). The highest measured tidal elevation at Wachapreague during 1996–2000 is 2.02 m while the highest predicted tide was just 1.02 m. The distribution of water superelevation or storm surge (measured minus predicted flood tide peak water level) as a function of wind direction (Figure 13, right) indicates the highest values are associated with winds from the NNW–NE sector, with a secondary peak for winds from the south. The maximum elevation of 2.02 m (5 February 1998; tidesandcurrents.-noaa.gov) was recorded during a northeasterly wind event (mean direction 27°) with wind speeds at NDBC buoy

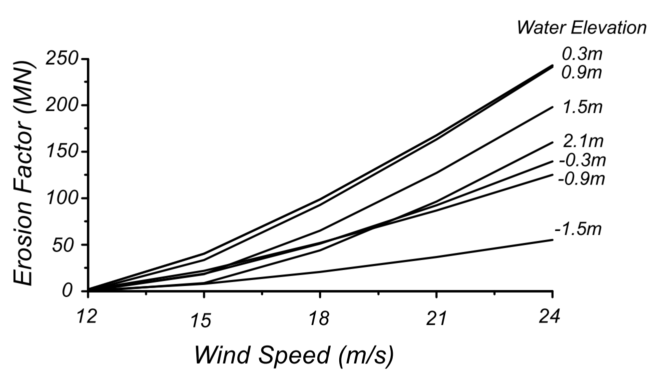

Figure 12. Erosion factor (equation (10)) as a function of wind speed from the north for different water elevations.

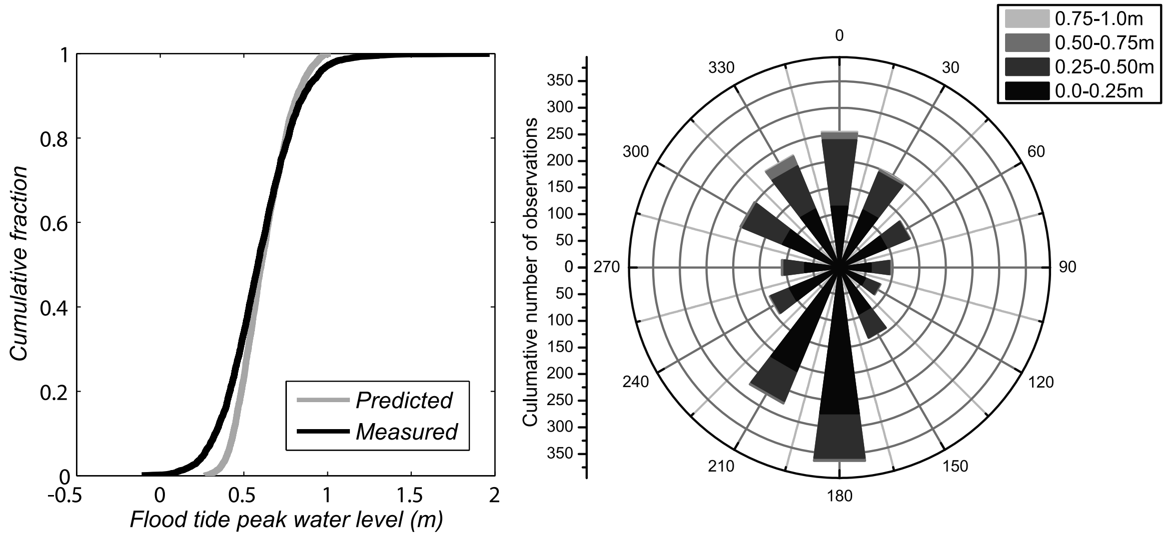

Figure 13. (left) Cumulative distribution of predicted and measured flood tide peak water level at Wachapreague, Virginia, during 1996–2000. (right) Directional distribution of the difference between measured and predicted flood tide peak water levels at Wachapreague, Virginia, during 1996–2000; only higher-than-predicted water levels are depicted here. Wind data are from NOAA buoy CHLV2 (compare Figure 2).

CHLV2 averaging 12 m s^{-1} over the course of 5.5 days; peak wind speed was 16 m s^{-1}.

[33] Water elevations between 0.2 and 1.0 m above MSL, the elevations with the highest erosion factors, occur about a third of the time in the study area. However, these water elevations were accompanied by wind speeds $\geq$15 m s^{-1} or higher less than 2% of the time ($\sim$5% for winds $\geq$11.2 m s^{-1}, one standard deviation above the mean). If we focus on wind events, defined here as intervals with peak wind speed $\geq$15 m s^{-1} and a minimum wind speed of 11.2 m s^{-1}, we find that mean event duration was 15 h (mode $\sim$ 13 h), indicating that the majority of storms extend through at least one full tidal cycle. Thus, during large storms, water levels are likely to fall within the range associated with the largest erosion factors as they ebb and flood. Tidal current velocities in these cases will be higher than they would be if these water elevations were reached closer to high-tide slack water conditions and the increased tidal prism associated with a storm surge further contributes to tidal velocities. Higher tidal velocities will increase fluxes of wave-resuspended sediment.

[34] The question remains of how well correlated wind speed, direction and water level superelevation are. Over the period from 1996 to 2000, storm surge at the Wachapreague tide gauge was significantly correlated with air pressure ($r = -0.38$) and along-peninsula wind speed ($r = 0.35$). From the perspective of wind events, storm surge averaged 0.30 m above predicted water levels when wind speeds were $\geq$15 m s^{-1}, compared to an average value of 0.06 m for all wind conditions. The distribution of mean wind direction for storm surge events has a primary peak in the northeasterly direction and a secondary peak for winds from the south (Figure 13, right).

6. Discussion

[35] Our methodology provides a simple estimate of the aggregate response of a shallow tidal basin to wind events, quantified in terms of an erosion factor, without the need to resolve each landscape unit separately. This method can be used to investigate the response of a particular tidal basin to wind wave-generated shear stresses and to provide a quantitative assessment of the impact of sea level rise (see below) or changes in sediment properties (e.g., due to changes in sediment supply or anthropogenic modifications of the coastline) on erosion potential. The method also provides a useful tool for quantitative comparison of basins with varying intertidal landscape complexity, sediment properties, tidal range, storm surge and/or sea level rise.

[36] Our application of the method to the shallow coastal bays of the Virginia Coastal Reserve reveals that wind waves produce four bottom shear stress regimes depending on water elevation, a result that is likely to apply generally to shallow tidal basins. For water elevations below MLLW (subtidal regions), increases in fetch and wave height are associated with increases in water level, so that average bottom shear stress does not significantly change with depth. For elevations between MLLW and MSL (tidal flats) an increase in water depth reduces bottom shear stresses while wave height increases only slowly. For elevations between MSL and MHHW, the elevation range in which most tidal salt marshes are found [*Morris et al.*, 2002], salt marshes become flooded thus increasing the average fetch. In this elevation range the height of the waves increases more than the depth producing a peak in average bottom shear stress and, as a consequence, a high potential for sediment resuspension. Within these elevations bottom shear stresses are controlled by fetch. Finally, for elevations above MHHW and therefore typical of storm surges, the fetch remains essentially constant and wave heights increase more slowly than water depth, thus reducing the average bottom shear stress. Therefore in this elevation range the bottom shear stresses are controlled by depth. The reduction of shear stresses during large storm surges can reduce the

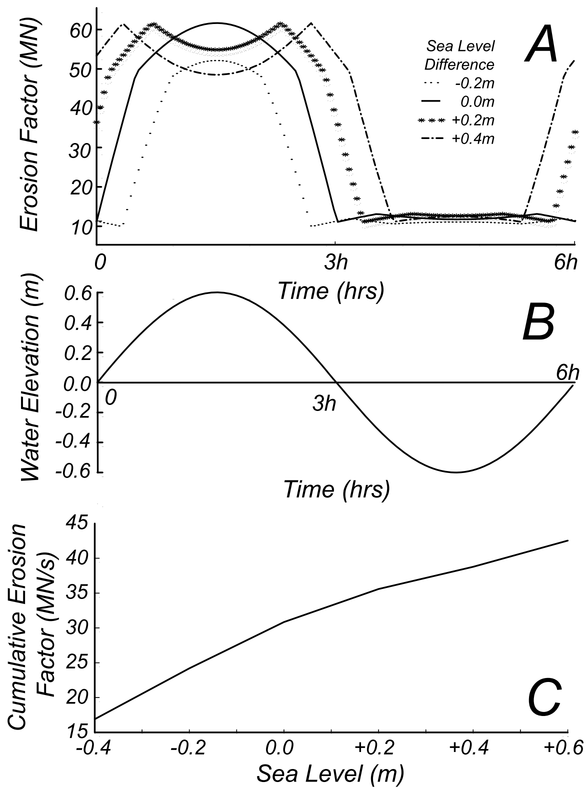

Figure 14. Erosion factor as a function of tidal elevation for different scenarios of sea level elevation: (a) erosion factor in a tidal cycle for a wind of 15 m s^{-1} blowing from NNE, (b) representative tidal cycle utilized to compute the erosion factor, and (c) cumulative erosion factor (average erosion factor in a tidal cycle) as a function of sea level elevation.

impact of hurricanes and extratropical storms on basin bottom morphology (but not at the basin margins).

[37] To explore the effect of changing sea level, we calculated erosion factor as a function of time (Figure 14a) during a sinusoidal tidal cycle with a 12 h period and range of 1.2 m (Figure 14b) for mean sea level elevations ranging from −0.2 m to +0.4 m; winds were 15 m s^{-1} from the NNE. These different scenarios could represent either long-term sea level rise or short-term storm surge during which wind setup is superimposed on tidal oscillations. The cumulative erosion factor (average value during a tidal cycle) is reported in Figure 14c as a function of sea level. When water elevation is too high, the erosion factor, and therefore sediment resuspension, drops as in the > MHHW regime of Figure 9. This notwithstanding, the cumulative erosion factor increases monotonically with sea level/storm surge elevation (Figure 14c). Since the sediment exiting the basin through the inlets is related to the amount of material resuspended [e.g., *Tambroni and Seminara*, 2006], our method can also provide important information for the determination of sediment fluxes to the ocean as a function of intertidal morphology. Moreover we can deduce that an increase in sea level would augment sediment resuspension in the basin under normal tidal conditions, assuming invariant basin morphology. In reality, changes in landform distribution produced by sea level oscillations can modify the erosion factor and therefore sediment resuspension.

[38] It is important to note that our method determines only the potential sediment erosion or resuspension and not the total amount of sediment in the water column. Sediment concentration is also a function of tidal currents that redistribute the material in the basin and sediment deposition, which extracts particles from the water column. Moreover, large values of substrate erosion modify bottom morphology, thus changing water depths and shear stresses. The erosion factor *EF* is thus valid only for erosion ranges from millimeters to centimeters of substrate.

[39] The results presented herein are in accordance with the conceptual model of *Fagherazzi et al.* [2006] [see also *Fagherazzi et al.*, 2007; *Defina et al.*, 2007]. Following *Fagherazzi et al.* [2006], tidal flats in shallow basins can accrete until a critical depth, above which they become unstable and evolve into salt marshes. The critical depth corresponds to the maximum bottom shear stress produced by wind waves, which, by eroding the bottom substrate, maintain the tidal flat below mean sea level. Here we show that the maximum bottom shear stresses occur for wind events that occur when the marshes are flooded, with sediment resuspension mostly occurring on the tidal flats. These events are the chief mechanism that maintains the tidal flats in equilibrium below mean sea level, rather than waves that develop during average or low water elevations.

[40] The conceptual model presented by *Fagherazzi et al.* [2006] of the factors controlling the boundary between tidal flats and salt marshes and our calculations of erosion potential do not account for the effects of vegetation on tidal flats. Sea grasses, once common in the Virginia Coast Reserve and recently reintroduced in these shallow lagoons after a 70-year absence [*Orth et al.*, 2006], can play a critical role in the stabilization of the tidal flat substrate as well as on its equilibrium elevation by increasing the bed shear stresses required to resuspend bottom sediment and dampening wave energy [*Fonseca and Fisher*, 1986; *Fonseca and Cahalan*, 1992]. Propagation of halophyte vegetation from salt marshes onto accreting intertidal flats is another mechanism that could decrease erosion potential but is not accounted for in our calculations.

[41] Our results underline the importance of salt marshes for protecting tidal flats from wind wave erosion. Without salt marshes, the fetch would be much larger for water elevations near MSL for winds from all directions, thereby increasing wave heights and the erosion factor over large portions of the tidal cycle.

[42] The preliminary results presented herein should be interpreted with caution. The framework presented by *Young and Verhagen* [1996a] is valid for shallow basins with flat bottoms, whereas sudden bathymetric changes associated with channels, tidal flats and salt marshes can strongly influence the development of wind waves. More refined models, based on production and dissipation of wave energy [e.g., *Carniello et al.*, 2005; *Booij et al.*, 1999] could improve the description of wind wave generation, though to our knowledge a wave model explicitly developed from extensive wave data sets in shallow coastal bays is still unavailable. Moreover, given the sensitivity of fetch and wave height to basin topography, high-resolution bathymetry with precision at the centimeter scale is necessary to accurately

calculate the distribution of wind wave-generated bottom shear stresses in shallow tidal basins. Unfortunately, few such data sets are available owing to the difficulty of reaching shallow areas using instrumented boats and the alternation of submerged and subaerial landforms that complicates topographic extraction from remote sensing. Finally, a validation of the shear stress equations with wave data in the Virginia Coast Reserve is clearly needed and will be addressed in future research.

7. Conclusions

[43] We present herein a simple method to determine the aggregate response of a shallow tidal basin to wind wave events. Application of the method produces spatially integrated values of erosion potential for the entire basin caused by wave activity as a function of tidal elevation, wind speed, and directionally dependent fetch. Calculated values of the integrated erosion potential, quantified as an erosion factor, can be compared to the sediment export to the ocean through the inlets and to the sediment supply from incoming rivers. Moreover, this holistic approach provides researchers a means to quickly determine the response of an entire system to disturbances such as sea level rise, anthropogenic modifications (e.g., dredging and nourishment), and climate driven variations in storm frequency and intensity.

[44] The response of a tidal basin to wind events is shown to be sensitive to wind direction relative to basin geometry and water elevation. On the basis of our application of the method to the Virginia Coast Reserve barrier-lagoon-marsh complex, which is typical of many shallow coastal bay systems, we identified four distinct regimes of wave-generated bottom shear stress and erosion potential as a function of water elevation.

[45] 1. For water elevations below MLLW (subtidal areas), an increase in fetch and therefore wave height is counteracted by an increase in depth, so that the average bottom shear stress is maintained constant as water depth varies because of tidal oscillations.

[46] 2. For elevations between MLLW and MSL (tidal flats) the increase in water depth dominates the increase in wave height thus reducing the bottom shear stresses. The system is therefore depth driven, meaning that water depth plays a critical role on the magnitude of bottom shear stresses.

[47] 3. For elevations between MSL and MHHW, the range associated with stable salt marsh platforms, flooding of the salt marshes increases fetch, wave height and bottom shear stresses, producing the largest potential erosion. The system is fetch driven, meaning that fetch plays a critical role on the magnitude of bottom shear stresses.

[48] 4. For elevations above MHHW, which are often associated with storm surge, intertidal landforms are submerged and increases in depth reduce average bottom shear stresses and potential erosion in the tidal basin. The system is therefore depth driven.

[49] Finally, simulations with increasing sea level show that the potential erosion monotonically increases with sea level elevation, thus most likely leading to morphological change in shallow intertidal basins under current scenarios of climate change.

[50] **Acknowledgments.** This research was supported by the Department of Energy NICCR program award TUL-538-06/07, by NSF through the VCR-LTER program award GA10618–127104, and by the Office of Naval Research award N00014-07-1-0664. The comments of three reviewers and the Associate Editor significantly improved the paper.

References

Amos, C. L., A. Bergamasco, G. Umgiesser, S. Cappucci, D. Cloutier, L. DeNat, M. Flindt, M. Bonardi, and S. Cristante (2004), The stability of tidal flats in Venice Lagoon: The results of in-situ measurements using two benthic, annular flumes, *J. Mar. Syst.*, *51*(1–4), 211–241, doi:10.1016/j.jmarsys.2004.05.013.

Booij, N., R. C. Ris, and L. H. Holthuijsen (1999), A third-generation wave model for coastal regions: 1. Model description and validation, *J. Geophys. Res.*, *104*(C4), 7649–7666, doi:10.1029/98JC02622.

Bretschneider, C. L. (1958), Revisions in wave forecasting: Deep and shallow water, paper presented at 6th International Conference on Coastal Engineering, Am. Soc. of Civ. Eng., Gainesville, Fla.

Carniello, L., A. Defina, and S. Fagherazzi (2005), A combined wind wave-tidal model for the Venice Lagoon, Italy, *J. Geophys. Res.*, *110*, F04007, doi:10.1029/2004JF000232.

Coastal Engineering Research Center (CERC) (1984), *Shore Protection Manual*, U.S. Army Coastal Eng. Res. Cent., Vicksburg, Miss.

Defina, A., L. Carniello, S. Fagherazzi, and L. D'Alpaos (2007), Self-organization of shallow basins in tidal flats and salt marshes, *J. Geophys. Res.*, *112*, F03001, doi:10.1029/2006JF000550.

Fagherazzi, S., and I. Overeem (2007), Models of deltaic and inner continental shelf landform evolution, *Annu. Rev. Earth Planet. Sci.*, *35*, 685–715, doi:10.1146/annurev.earth.35.031306.140128.

Fagherazzi, S., A. Bortoluzzi, W. E. Dietrich, A. Adami, S. Lanzoni, M. Marani, and A. Rinaldo (1999), Tidal networks: 1. Automatic network extraction and preliminary scaling features from digital terrain maps, *Water Resour. Res.*, *35*(12), 3891–3904, doi:10.1029/1999WR900236.

Fagherazzi, S., L. Carniello, and A. Defina (2006), Critical bifurcation of shallow microtidal landforms in tidal flats and salt marshes, *Proc. Natl. Acad. Sci. U. S. A.*, *103*(22), 8337–8341, doi:10.1073/pnas.0508379103.

Fagherazzi, S., C. Palermo, M. C. Rulli, L. Carniello, and A. Defina (2007), Wind waves in shallow microtidal basins and the dynamic equilibrium of tidal flats, *J. Geophys. Res.*, *112*, F02024, doi:10.1029/2006JF000572.

Fitzgerald, D. M., M. Kulp, S. Penland, J. Flocks, and J. Kindinger (2004), Morphologic and stratigraphic evolution of muddy ebb-tidal deltas along a subsiding coast: Barataria Bay, Mississippi River delta, *Sedimentology*, *51*(6), 1157–1178, doi:10.1111/j.1365-3091.2004.00663.x.

Fitzgerald, D. M., M. S. Fenster, B. A. Argow, and I. V. Buynevich (2008), Coastal impacts due to sea-level rise, *Annu. Rev. Earth Planet. Sci.*, *36*, 601–647, doi:10.1146/annurev.earth.35.031306.140139.

Fonseca, M. S., and S. S. Bell (1998), Influence of physical setting on seagrass landscapes near Beaufort, North Carolina, USA, *Mar. Ecol. Prog. Ser.*, *171*, 109–121, doi:10.3354/meps171109.

Fonseca, M. S., and J. A. Cahalan (1992), A preliminary evaluation of wave attenuation by four species of seagrass, *Estuarine Coastal Shelf Sci.*, *35*(6), 565–576, doi:10.1016/S0272-7714(05)80039-3.

Fonseca, M. S., and J. S. Fisher (1986), A comparison of canopy friction and sediment movement between four species of seagrass with reference to their ecology and restoration, *Mar. Ecol. Prog. Ser.*, *29*, 15–22, doi:10.3354/meps029015.

Fredsoe, J., and R. Deigaard (1993), *Mechanics of Coastal Sediment Transport*, *Adv. Ser. Ocean Eng.*, vol. *3*, 392 pp., World Sci., Singapore.

Hasselmann, K., et al. (1973), Measurements of wind-wave growth and swell decay during the Joint North Sea Wave Project (JONSWAP), *Dtsch. Hydrogr. Z.*, *8*(12), 1–95.

Hayden, B. P., C. F. V. M.Santos, G. Shao, and R. C. Kochel (1995), Geomorphological controls on coastal vegetation at the Virginia Coast Reserve, *Geomorphology*, *13*(1–4), 283–300, doi:10.1016/0169-555X(95)00032-Z.

Huang, W., H. Sun, S. Nnaji, and W. K. Jones (2002), Tidal hydrodynamics in a multiple-inlet estuary: Apalachicola Bay, Florida, *J. Coastal Res.*, *18*(4), 674–684.

Kamphuis, J. W. (1975), Friction factor under oscillatory waves, *J. Waterw. Harbors Coastal Eng. Div. Am. Soc. Civ. Eng.*, *101*, 135–144.

Knutson, P. L., R. A. Brochu, W. N. Seelig, and M. Inskeep (1982), Wave damping in Spartina alterniflora marshes, *Wetlands*, *2*(1), 87–104.

Lawson, S. E. (2004), Sediment suspension as a control on light availability in a coastal lagoon, M.S. thesis, 117 pp., Univ. of Va., Charlottesville.

Lawson, S. E. (2008), Physical and biological controls on sediment and nutrient fluxes in a temperate lagoon, Ph.D. dissertation, 187 pp., Univ. of Va., Charlottesville.

Lawson, S. E., P. L. Wiberg, and K. J. McGlathery (2007), Wind-driven sediment suspension controls light availability in a shallow coastal lagoon, *Estuaries Coasts*, *30*(1), 102–112.

Möller, I., T. Spencer, and J. R. French (1996), Wind wave attenuation over saltmarsh surfaces: Preliminary results from Norfolk, England, *J. Coastal Res.*, *12*(4), 1009–1016.

Möller, I., T. Spencer, J. R. French, D. J. Leggett, and M. Dixon (1999), Wave transformation over salt marshes: A field and numerical modelling study from North Norfolk, England, *Estuarine Coastal Shelf Sci.*, *49*(3), 411–426, doi:10.1006/ecss.1999.0509.

Morris, J. T., P. V. Sundareshwar, C. T. Nietch, B. Kjverve, and D. R. Cahoon (2002), Responses of coastal wetlands to rising sea level, *Ecology*, *83*(10), 2869–2877.

Oertel, G. F. (2001), Hypsographic, hydro-hypsographic and hydrological analysis of coastal bay environments, Great Machipongo Bay, Virginia, *J. Coastal Res.*, *17*(4), 775–783.

Orth, R. J., M. L. Luckenbach, S. R. Marion, K. A. Moore, and D. J. Wilcox (2006), Seagrass recovery in the Delmarva Coastal Bays, USA, *Aquat. Bot.*, *84*(1), 26–36, doi:10.1016/j.aquabot.2005.07.007.

Precht, E., and M. Huettel (2003), Advective pore-water exchange driven by surface gravity waves and its ecological implications, *Limnol. Oceanogr.*, *48*(4), 1674–1684.

Precht, E., U. Franke, L. Polerecky, and M. Huettel (2004), Oxygen dynamics in permeable sediments with wave-driven pore water exchange, *Limnol. Oceanogr.*, *49*(3), 693–705.

Ramage, D. L., and D. R. Schiel (1999), Patch dynamics and response to disturbance of the seagrass Zostera novazelandica on intertidal platforms in southern New Zealand, *Mar. Ecol. Prog. Ser.*, *189*, 275–288, doi:10.3354/meps189275.

Rodriguez-Iturbe, I., and A. Rinaldo (1997), *Fractal River Basins: Chance and Self-Organization*, 546 pp., Cambridge Univ. Press, Cambridge, U. K.

Sanford, L. P., and J. P. Y. Maa (2001), A unified erosion formulation for fine sediments, *Mar. Geol.*, *179*(1–2), 9–23, doi:10.1016/S0025-3227(01)00201-8.

Tambroni, N., and G. Seminara (2006), Are inlets responsible for the morphological degradation of Venice Lagoon?, *J. Geophys. Res.*, *111*, F03013, doi:10.1029/2005JF000334.

Thijsse, J. T. (1949), Dimensions of wind-generated waves, paper presented at General Assembly of Association d'Oceanographie Physique, Oslo.

U.S. Army Corps of Engineers (1955), Waves and wind tides in shallow lakes and reservoirs, *Summary Rep. Proj. CW-167*, Jacksonville, Fla.

Vallino, J. J., and C. S. Hopkinson (1998), Estimation of dispersion and characteristic mixing times in Plum Island Sound estuary, *Estuarine Coastal Shelf Sci.*, *46*(3), 333–350, doi:10.1006/ecss.1997.0281.

Young, I. R., and L. A. Verhagen (1996a), The growth of fetch limited waves in water of finite depth. 1. Total energy and peak frequency, *Coastal Eng.*, *29*(1–2), 47–78, doi:10.1016/S0378-3839(96)00006-3.

Young, I. R., and L. A. Verhagen (1996b), The growth of fetch limited waves in water of finite depth. 2. Spectral evolution, *Coastal Eng.*, *29*(1–2), 79–99, doi:10.1016/S0378-3839(96)00007-5.

S. Fagherazzi, Department of Earth Sciences, Boston University, Boston, MA 02215, USA. (sergio@bu.edu)

P. L. Wiberg, Department of Environmental Sciences, University of Virginia, Charlottesville, VA 22904, USA.